Development of an Advanced Control Algorithm for DAB DC/DC Converters: Inrush Current Limitation and Enhanced Operation in Transient States

Serafin Bachman[1] Marek Turzyński[2]

[1] Politechnika Warszawska, Instytut Sterowania i Elektroniki Przemysłowej
[2] Politechnika Gdańska, Katedra Energoelektroniki i Maszyn Elektrycznych

Abstract The publication addresses the dynamic state challenges encountered during development of a Dual Active Bridge (DAB) converter within DC microgrid systems. The conventional startup method is identified as instigating a cascade of unfavorable outcomes, encompassing elevated starting current, transformer current asymmetry, DC voltage distortions, EMI and heightened thermal stress on semiconductor components. Additionally, it necessitates precise calibration of magnetic components and diodes. A proposed remedy to these issues is introduced, involving a control method based on an additional phase shift to modulate the current of the primary H bridge. This novel control methodology is posited as a means to mitigate the aforementioned undesirable effects associated with traditional converter initiation techniques. The research also delves into considerations of proper design procedure for the converter. Emphasis is placed on integrating the novel control methodology into the design framework to effectively address challenges arising during transient states. Validation of the proposed solution is substantiated through a series of laboratory tests, the results of which are comprehensively presented in the article. These tests affirm the efficiency of the system when incorporating the novel control methodology, thereby substantiating its practical utility in mitigating the identified issues during the initiation phase of the DAB converter in DC microgrid systems.

Key words: Dual active bridge, bidirectional isolated DAB, efficiency, control loop, transient state problems, analytical calculations, DC/DC converter

1. INTRODUCTION

The significance of DC microgrids is steadily increasing. This trend is driven by the growing integration of renewable energy sources, electric vehicle charging systems, and energy storage systems into a unified network, driven by the rising energy demand. As stated in [1], the number of devices connected to such networks is growing annually, and this trend is expected to continue.

It is essential to recognize that in the DC microgrid (DC-MG) microsystem, the energy sources and loads have the ability to operate at various voltage levels, as emphasized in [2]. Moreover, certain power sources, such as wind generators, and certain receivers inherently operate on alternating voltage. As a result, to facilitate their integration into the main DC bus, both receivers and power sources require connection through suitable power electronic converters. This adaptation is crucial to harmonize the different voltage characteristics of these components with the DC microgrid infrastructure.

In the context of energy storage facilities, which encompass battery banks and supercapacitor banks, an additional consideration arises: the necessity to enable bidirectional energy flow. This bidirectional flow involves transferring energy from the bus to the storage unit during the charging mode and vice versa, from the storage unit back to the bus during energy recovery mode. This bidirectional capability ensures the flexibility required for optimal energy management within the DC microgrid, accommodating the dynamic needs of both energy storage and retrieval processes.

An isolated DC/DC energy conversion stage is vital for the operation of many systems. The most popular solution, employed in various applications such as chargers for electric vehicles [2]-[3], novel traction solutions [4], microgrid systems [5], and integrated energy storage systems [6], utilizes a Dual Active Bridge (DAB) converter. This converter is characterized by high power density, achieving peak efficiency of about 98% [7], and providing galvanic isolation. The schematic of the DAB is depicted in Figure 1.

The inherent advantages of DAB systems encompass a range of crucial attributes, solidifying their standing across diverse applications [8]:

Simplicity of Structure: DAB systems feature an inherently uncomplicated architectural design, facilitating straightforward implementation and maintenance.

Exceptional Efficiency: With a noteworthy efficiency quotient of up to 98%, DAB systems underscore their

proficiency in energy conversion, minimizing losses and enhancing overall operational efficacy.

Bidirectional Energy Transfer with Unified Control Strategy: A key strength of DAB systems lies in their adept facilitation of bidirectional energy transfer. Notably, this capability is accompanied by a uniform control strategy, regardless of the direction of energy flow, providing heightened operational versatility.

Power Density: DAB systems distinguish themselves with a superior specific power density, delivering substantial power outputs relative to their physical dimensions and weight.

Soft Switching Capability: The engineering ingenuity of DAB systems allows for the implementation of soft switching methodologies for the system's transistors, mitigating switching losses and enhancing overall efficiency.

Minimal Passive Elements: DAB systems are characterized by an economy of passive elements, presenting a streamlined configuration that bolsters system reliability while mitigating complexities associated with an excess of passive components.

Galvanic Isolation: A critical attribute of DAB systems lies in the provision of galvanic isolation between the input and output of the converter. This feature engenders electrical segregation between distinct sections of the system, addressing concerns pertaining to safety and operational integrity.
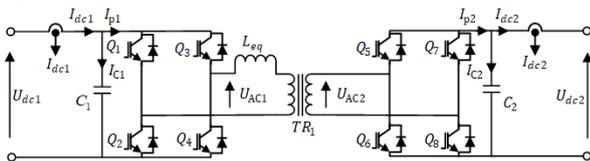

Fig.1. Dual Active Bridge (DAB) scheme

DAB converters encounter challenges in both dynamic and static operational states, contingent on the selected parameters and control strategies. Particularly, erroneous selection of magnetic components may trigger issues such as sags or polarity reversals of the phase voltage. These problems arise when the rising edge time of the current is too short relative to the drift factor [9], resulting in reactive power transfer flow. Proper selection of magnetic components can mitigate this issue.

During dynamic states, another problem arises with dead time [10], which distorts the DC output voltage, especially noticeable during startup and step changes in phase shift. This distortion negatively affects the formation of the secondary side DC voltage, impacting the operation of other components in the microgrid system.

Furthermore, the voltage of the DC link influences the operation of all other connected circuits, increasing their losses and reducing the nominal lifetime of the devices used. The lifetime of converter strictly depends on the method of converter start and dynamic states [11], due to the delta temperature of semiconductors, leading to their gradual degradation.

A sudden voltage spike can abrupt response from the control system, manifesting as a current surge. This phenomenon adversely affects the lifetime of converter, particularly rectifier diodes subjected to a surge in current [12].

A combination of these problems contributes to problems with microgrid stability, among other issues. When the microgrid is stable after being subjected to a disturbance, all state variables recover to (possibly new) steady state values which satisfy operational constraints (e.g.: load changer, component failure, change of setpoints) [13].

The presented work focuses on proposing a control model that addresses the design procedure to eliminate problems such as high inrush current, current surges of semiconductor components, current asymmetry, and transformer saturation. This article makes a significant contribution by providing a comprehensive analysis of the identified problems. Moreover, it introduces a novel approach to address these issues through the implementation of a compensatory method during the converter startup phase. This involves utilizing a meticulously designed magnetic circuit and incorporating a contemporary technique for shaping the secondary side voltage.

The significance of this contribution lies in its dual focus: firstly, in thoroughly dissecting the problem at hand, and secondly, in proposing a solution that integrates both a refined magnetic circuit design process and a cutting-edge approach to voltage shaping on the secondary side. By doing so, the article not only advances our understanding of the identified issue but also offers a tangible and innovative means to rectify it. This two-way contribution aims to enhance the efficiency and performance of the converter, thereby making a notable impact within the realm of power electronics.

2. DESIGN PROCEDURE

Classically, the parameters of DAB are selected based on the following parameters: switching frequency, series inductance, dead time, control strategy, power cycle characteristic, and voltage ratio. A classic schematic of DAB converter is shown in Figure 1.

In the classic variant, the parameter selection order is not considered. Based on the adopted voltage ratio and output power, the value of the series inductance is calculated using the ideal output power equation. The transformer is selected so that it works with a 1:1 ratio at the nominal operating point and can withstand the nominal power multiplied by a factor of 1.3 – 1.5 [14].

That solution causes many problems that can be completely or partially omitted based on the current state of knowledge. Examples of issues that can be avoided to a large extent include incorrect calculation of the phase shift for a given output power value[15]. This problem is resulting from the assumption of an ideal power characteristic. Other possible problems to solve refer to: switching when the system is operated with a small phase shift value, significant current distortion by DC offset resulting from too low saturation current of the transformer and lack of compensation for this effect in the control, and significant reduction of the system lifetime by subjecting it to frequent temperature delta changes due to the wrongly selected transformer voltage ratio [14]. These and many other problems can be ruled out if the correct design procedure is followed.

2

The proposed procedure, taking into account the phenomena related to the problems of dead time, transformer current asymmetry, and non-linear characteristics of the system operation, what is shown in Figure 2. It represents a state machine that determines correct parameter values according to a predetermined order. The leakage inductance selection depends on the result of the dead time drift.
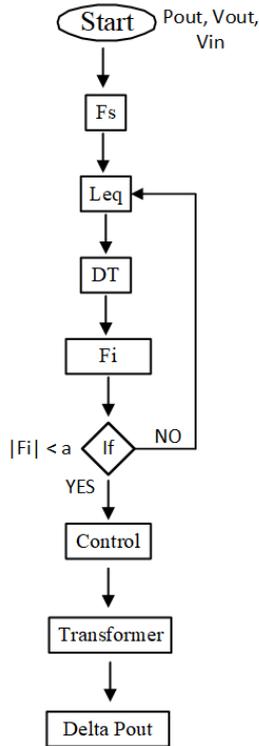

Fig.2. Proposed design procedure of the Dual Active Bridge. Where *Fs* is a switching frequency, *Leq* is series inductance, *Fi* is a phase shift, *a* is a dead time drift factor, *DT* is a dead time,

The presented design procedure is based on the assumption of designing equipment in which there are no issues with dead time drift, damage in dynamic states, and significant current surges. By employing this design methodology, the reliability of the designed system is enhanced.

The procedure involves determining the values of rated power and voltages; based on these values, semiconductor elements are selected along with the system operating frequency. Subsequently, the value of series inductance is determined for ideal conditions. In the next step, the dead time value is chosen based on the derived system operating range in ZVS (Zero Voltage Switching). Considering the dead time and ZVS range, the phase shift range in which the system will operate is determined. If this range is unsatisfactory or there is an issue, such as the resolution of the phase shift in a given range allowing for dead time drift, one must return to the selection of the series inductance value and modify it, proceeding to the subsequent steps. With these well-chosen parameters, it is possible to design the control loop in accordance with application requirements and design the magnetic circuit. Based on the final calculated parameters and system heating tests, the maximum possible operating range should be determined.

The calculation of the dead-time drift condition is done using equations 1 and 2 which describe the relation between the dead time T_{DT} and the switching period T_{SW} for the given voltage ratio k_u, where n is transformer ratio and $Udc1$ and $Udc2$ are primary and secondary DC voltage.

$$a = \frac{2T_{DT}}{T_{SW}} \quad for \quad k_u > 1 \qquad (1)$$

$$a = \frac{-2T_{DT}}{T_{SW}} \quad for \quad k_u < 1 \qquad (2)$$

$$k_u = \frac{nU_{dc2}}{Udc1} \qquad (3)$$

For the considered variant in this publication, with a dead time of 100ns and a switching frequency of 50kHz, based on the equations 1 and 2, the recommended range to avoid in control is the interval <-0.01; 0.01>. It is possible to skip this range by using a phase shift resolution greater than 0.01 or by introducing a phase shift limitation within this range. Based on these options, we assume that a better solution would be to implement a phase shift limitation within this range. A solution involving limiting the resolution of the control signal so that the step of phase shift is greater than the dead time drift may lead to a deterioration of system stability in some cases.

The classic procedure focuses on the ideal model of the converter and therefore does not take into account phenomena affected by the DAB losses.

The proposed approach in Figure 2 considers more detailed characteristics, own control solutions, and improvement of problems with dynamic states. These issues will be discussed in more detail later in this paper.

3. INRUSH ASYMMETRIC STARTUP CURRENT

Switching on the primary side bridge at zero secondary side voltage causes a high starting current, which cannot be shaped with the classic SPS (Single Phase Shift) control method. Typical waveforms of starting voltage and current are shown in Figure 3. The peak value of the inrush current requires re-scaling of the magnets to eliminate DC offset of the transformer current, as well as the selection of appropriately current-resistant rectifier diodes of the secondary side bridge. This problem has already been discussed in the literature [15].


Fig.3. Waveforms of typical SPS first starting pulses, voltage and current of the transformer outputs. DC voltage of secondary side is zero at that moment, due to that reason the secondary side voltage is starting to increase on each pulse, during capacitance charging.

Fig.4. Waveforms of typical soft start methods a) SPS traditional method with 20% of secondary current asymmetry b) SPS with minimal starting pulse with 18% of secondary current asymmetry c) SPS with 3 starting pulses with 25% of secondary current asymmetry

The proposed solutions do not solve all issues like related to circulating currents and generated reactive power. and often, by adding a very advanced modulator algorithm, e.g., TPS (Tripple Phase Shift) [16], they unnecessarily complicate the control, thus preventing its implementation in DSP (Digital Signal Processor) and FPGA (Field Programed Gate Array) systems with low computing power.

The lack of voltage on the secondary side forces a high current in the secondary side transformer output. This current decreases as the DC link capacitor of the secondary side is charged. The problem with the current surge is the selection of appropriately durable rectifier diodes in the secondary side bridge. Based on the author's experience, the peak current of the diodes should be selected at 150% of the peak current of the entire load state of the system to compensate this starting current. Unfortunately, this causes the need to oversize the system and increases the cost of converter implementation.

The start of the converter with a typical PI control loop forces a significant phase shift between the phase voltages. Due to the significant voltage difference across the series inductance, the transformer current is forced high, causing transformer saturation and a DC offset in the phase current of the secondary bridge. This problem is classically solved by rescaling the transformer size [17]. Increasing the size of the magnetic elements results in a significant increase in the cost of converter implementation.

In Figure 4, three possible start-up methods for the converter using the classical SPS modulation method are presented.

The first method involves the classic start-up of the converter with SPS modulation, resulting in significant overshoot and current asymmetry of approximately 20%.

The second method involves limiting the first pulse to 50%. This allows for limiting the rise of peak current. However, there still exists a significant asymmetry phenomenon in the current during the first pulses, up to 18%.

The third method involves preparing several pulses with limited duty cycle. This solves the overshoot issue of current values, but nonetheless, the remaining current asymmetry amounts to 25%.

This methods can be achieved by reducing the pulse width or introducing additional phase shift between the bridge branches, or even increasing the dead time. They significantly limits the first current pulse to values lower by over 50%. However, this method does not exclude the occurrence of the DC bias – current asymmetry - phenomenon in the transformer current. Therefore, it introduces additional oscillations in the controller's operation. Peak current value is also not significantly reduced, it will undoubtedly affect the semiconductor's lifespan in the future.

These problems also translate into the deformation of the secondary side DC voltage. In the case of back-to-back operation with another converter in the DC microgrid, this effect will negatively affect the entire starting procedure of the system, contributing to unnecessary load of semiconductor components.

In the literature, there are known attempts to solve this problem, such as [18] – [19]. Unfortunately, the proposed solutions are not complete. Their authors only work with a current regulator in the linear range of the characteristic, without a hardware concept of system capacity charging. It causes the problem of charging capacity in a semiconductor-safe manner.

4. STARTING PROCEDURE OF DUAL ACTIVE BRIDGE

The proposed solution is based on the reconfigured control loop shown in Figure 5.

Fig.5. Proposed control loop of the Dual Active Bridge

4

The considered control loop comprises a basic current regulator, with the possibility of selecting another control element. A possible selection concerns the value of the filtered set current, as well as the voltage and power regulators. The choice of the second control element depends on the value of the smallest set current. The block marked as DPS+Soft start is a modulator block intended to control the width of the pulses by DPS (Double Phase Shift) modulations during start-up and dynamic states. It is assumed in the control loop that the filling of the base pulses is always 50%. The offset measurement values are filtered by a low pass filter. The selection of filter settings and the control loop are described in [20].

The basic idea of the procedure is shown in Figure 6. The start-up procedure is divided into three main stages: (1) loading the system capacitance by using the hardware current limiting system on the resistance; (2) starting the converter without load, with the use of the IV DPS modulation state; and (3) switching on the main switch and working with the load with the use of DPS modulation in case of transient states. These solutions will be discussed in more detail later in the article.
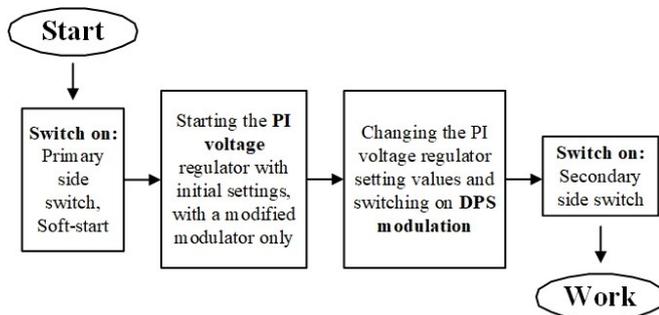
Fig.6. Basic starting procedure

The problem that needs to be solved in the hardware is related to initial charging of the converter capacitance when the power is turned on. This publication considers an actual DAB converter circuit with capacitance attached on both sides. For this reason, it is necessary to limit the high current pulse and operate the main switch. A schematic of that idea is shown in Figure 7.
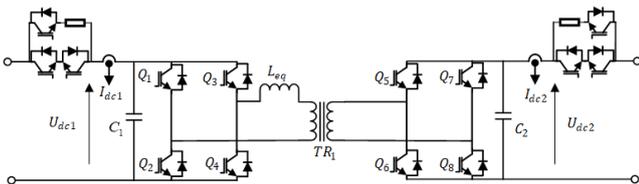
Fig.7. DAB with hardware soft start resistors

This solution stems from the necessity to create a universal system for use in microgrid systems, capable of having two different levels of phase voltages connected on the primary and secondary sides. Some form of isolation of the secondary side of the system for its startup is required, as well as the ability to charge significant capacitor capacitances in the DC circuit. In the absence of this

solution, a significant surge in capacitor charging current will be encountered. To mitigate this effect, a capacitor charging circuit is used through a simple resistor. Due to the current limitation of the resistor, a relay circuit is added in parallel. In this case, a circuit with a transistor featuring a low Rds(on) coefficient is employed to minimize losses to the maximum extent. Another possible option is to use a mechanical relay suitable for DC operation, but this significantly increases the cost of the device. Assuming the use of 4 transistors with a resistance of 4.5 mOhm and a peak current of 30A, we obtain losses at the level of 0.6W.

DPS modulation is well known and widely used in DAB systems. It has been discussed in [21], among other publications. This modulation can be divided into 6 key states, presented in Table I. In contrast to the traditional SPS modulation method, some of the used states have higher circulating currents, and full (ZVS) of transistors is not always obtained. Moreover, in the nominal operation state, the DPS modulation works with almost zero phase shifts between the bridge branches. What is also worth noting is the complexity of the entire DPS algorithm. The DPS control concept is presented in Figure 8.
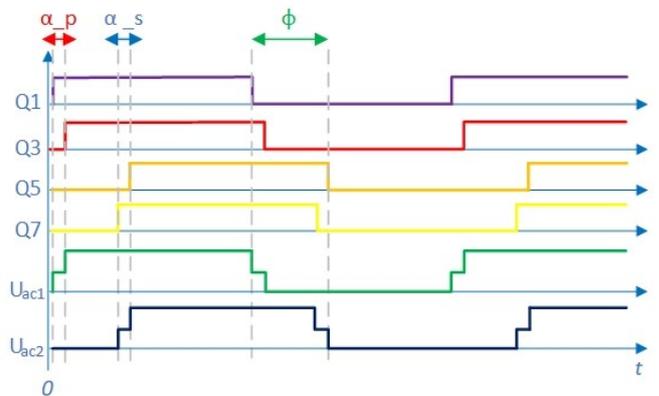

Fig.8. Possible waveforms achievable when using 3 phase shifts

TABLE I. DAB state comparison

State	Specification
Ia	ZVS only for $\varphi > 0$ Higher RMS current than in SPS
Ib	No ZVS Higher RMS current than in SPS
II	No ZVS
III	ZVS Higher RMS current than in SPS
IV	ZVS Limitation of circulating current Lower RMS current than in SPS Only for low power operation

The table presents various modulation state variants based on the DPS method. The term "state" refers to the operating point of the control method, based on the appropriate equations utilized in that state. The presented analysis was carried out based on [22]-[23]. As described in Table I, only state IV allows to obtain an advantage over the classic SPS

5

modulator in the full range. This solution is dedicated to work with low power. As already mentioned, this feature will be used to implement the control mainly to start the converter with no load attached.

After analyzing the part of DPS control of interest, the algorithm presented in Figure 9 was created. In this algorithm, φ means the phase shift calculated based on the DAB equation, M is modulation index, Fif is a phase shift vector position, Uzad is set voltage, Uref is a reference voltage od power supply AlphaP and AlphaS are additional phase shift calculated parameters added by DPS modulation.
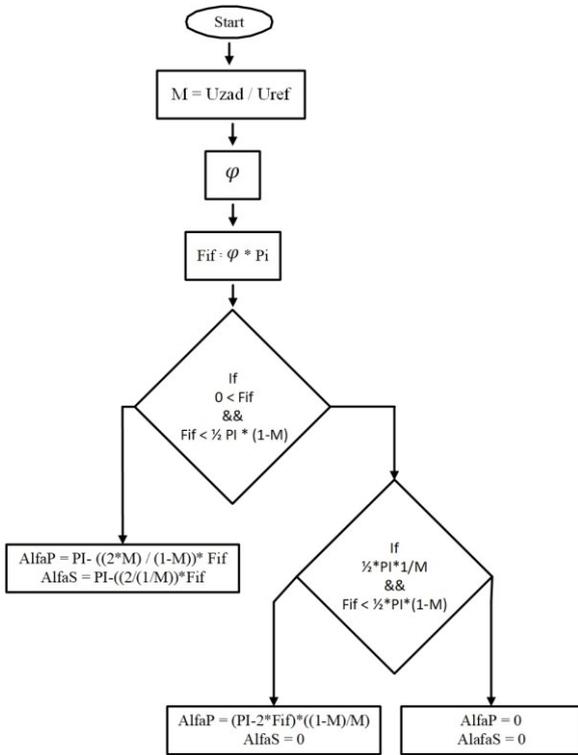
Fig.9. Dual phase shift algorithm
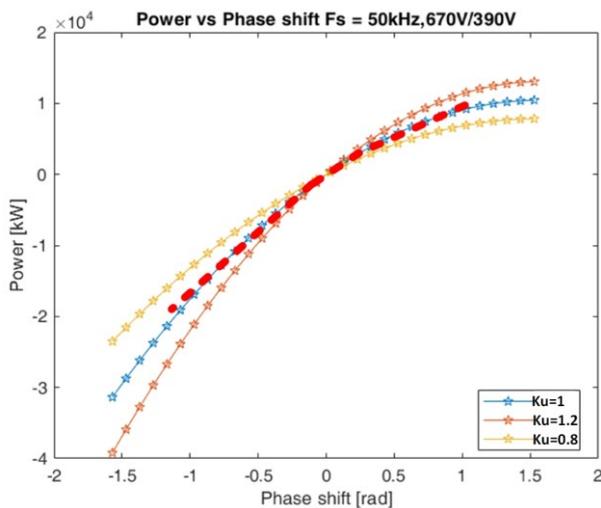
Fig.10. Nonlinear characteristic of DAB

Based on the previously conducted research and other publications [24], a nonlinear characteristic of the DAB

converter has been drawn, as shown in Figure 10. The characteristic is additionally marked with the information on the linearization of its fragments (red lines).

Due to the linear characteristic of the operation of the PI controller, it was decided to split the control loop into two separate controllers with different settings. The characteristics of these controllers, represented by red lines in Figure 10, enable linear operation of the control system. Based on the collected solutions, it is possible to shape the DAB phase waveforms, as shown in Figure 11. To limit sudden asymmetric current build-up.
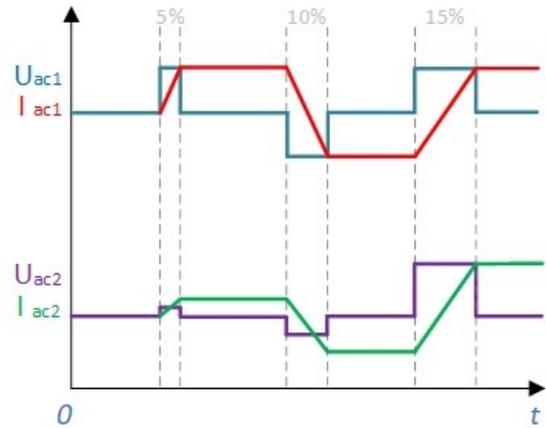
Fig.11. Theoretical shape of DAB phase voltage and current with percentage proportion of alfa phase shift parameter

5. Improvement of transient states

In the literature, the problem of transformer current asymmetry is known as resulting from the problem of sudden phase shift change which creates significant voltage difference on the inductor, forcing, as a consequence, high transformer current and causing its saturation and DC offset of the DAB phase current [25]. This current is discharged over time on the resistance of the transformer.

The above issue is known in the literature as L/R transient effect [26]. This problem has many solutions based on control and modulation [27] – [32].

In order to meet all the relevant criteria of the control model, a method of compensating these states has also been developed. This problem is largely solved by a correct design procedure which consist in the selection of appropriate magnetic components and the control method.

The control solution proposed in the paper makes use of changing additional phase shifts α_s and α_p in accordance with the DPS modulation principle. This offset is only added for a few operating periods after the transient state. Its definition is given in Figure 12.
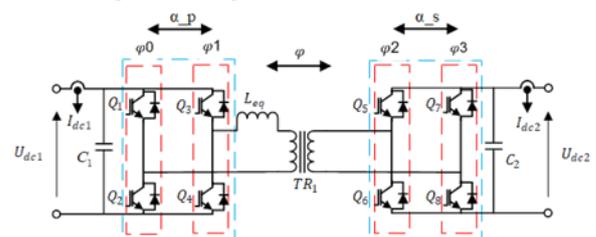

Fig.12. Definition of additional phase shift in the DPS concept

6

This solution makes it possible to limit the asymmetry of the phase current. It differs from the earlier solution used in DPS in that it is used only for phase shift step changes exceeding 30% and is implemented only for a few cycles. This solution is very easy to implement in FPGAs and can be easily tuned. Presented on Figure 13. Solutions of this type are known in the literature [22]. However, up to the present, they have not been included in the overall control loop including the converter start, control loops, and compensations of dynamic states for the DAB converter.
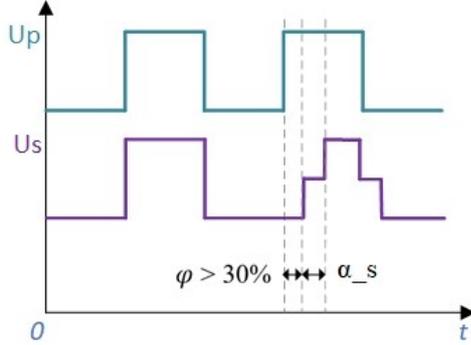
Fig.13. Theoretical shape of DAB phase voltage during transient state with additional α_S control

6. LABORATORY INVESTIGATION

The laboratory stand is shown in Figure 14. The laboratory setup parameters are presented in Table II.
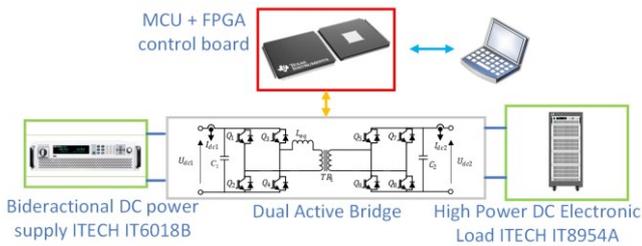
Fig.14. Laboratory stand schematic

TABLE II. DAB laboratory setup parameters

Parameter	Specification
Rated output power	10 kW
U_{DC1}	380 V
U_{DC2}	380 V
T_1-T_8, D_1 - D_8	F4-23MR12W1M1_B11 (Infineon) CoolSiC™ Trench MOSFET
Switching frequency	50 kHz
Power supply	ITECH60188
Transformer	3C95 ferrite core (SMA) O_D=87/I_D=56/H=50mm
L_d	25µH

Figure 15 illustrates the meticulously implemented waveforms that encapsulate the DAB start procedure. By applying the discussed method and appropriately adjusting the shape of the phase voltage on the primary side so that the duty cycle coefficient increases depending on the modulation index, two problems were completely eliminated. These problems include overcurrent on the primary and secondary sides as well as asymmetry in current waveforms. The presented waveforms indicate a nearly linear increase in the duty cycle coefficient in the examined case. With variable set and measured voltages, as well as variable secondary side voltage or load, the nature of these waveforms will change depending on these parameters.

a)

100us/div

b)
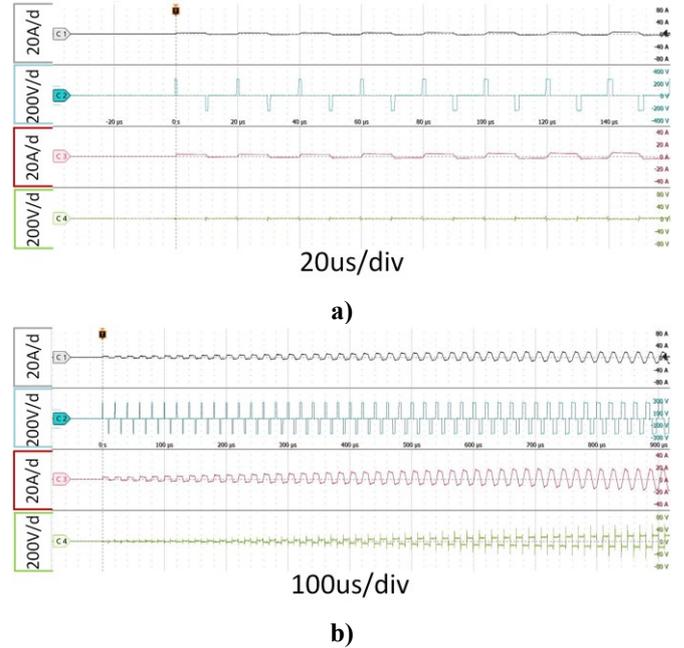
Fig.15. Proposed starting procedure of DAB a) micro perspective b) macro perspective. From top: primary phase current, primary phase voltage, secondary phase current, secondary phase voltage

When discussing Figure 15b, it is worth noting the occurrence of characteristic disturbances in the secondary side voltage resulting from the excitation of measurement devices. An important aspect is the shape of the current at the initial start stage, which is trapezoidal, and then, as the current on the secondary side increases, it takes on the characteristic triangular shape for the DAB system current in the idle state without load. The shape of the primary and secondary side voltages, when the rated voltage is reached, will take on a two-level rectangular shape.

Simultaneously, Figure 16 provides a comprehensive description of the principal effects discerned through the conducted control tests, featuring a typical initiation of a DAB converter. Within these curves, a conspicuous observation is the pronounced initial current surge, characterized by a distinct phase current offset. The main issue with these waveforms is the peak current reaching approximately 100 A. The tested system is designed to operate with currents three times smaller. This implies the necessity of using transistors with a current rating four times higher than the nominal value.

7
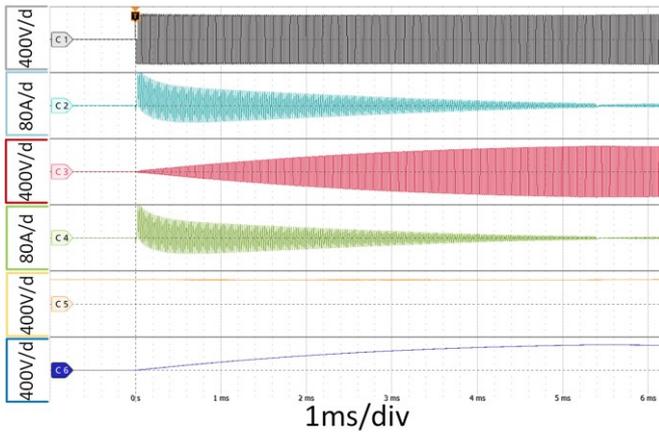
Fig.16. Classic DAB starting procedure based on SPS. From top: C1 - primary phase voltage, C2 - primary phase current, C3 - secondary phase voltage, C4 - secondary phase current, C5 - input supply DC voltage, C6 - output DC voltage

In contrast, Figure 17 presents the waveforms corresponding to a novel starting procedure. Notably, these waveforms demonstrate a controlled phase current during the initial 10 milliseconds, limited to the minimum requisite value for system initiation. Starting current without soft start (120A), with soft start and design procedure (20A). This comparative analysis highlights the efficiency of the new starting procedure in mitigating the abrupt current surge observed in traditional methods.
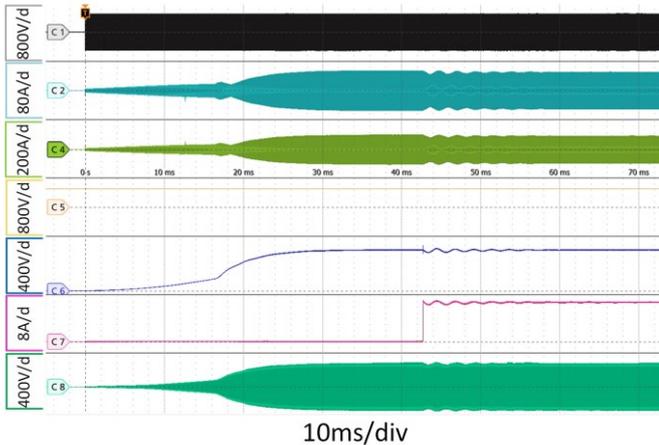
Fig.17. Result obtained with a new approach. From top: C1 - primary phase voltage, C2 - primary phase current, C4 - secondary phase current, C5 – input supply DC voltage, C6 – DC output voltage, C7- DC output current, C8 - secondary phase voltage

Figures 18a and 18b further delve into the comparative evaluation of the classic control method employing the DPS modulator, comparison with the concept of usage DPS IV state control method. These figures provide insights into the nuanced distinctions between the two control methodologies. The presented waveforms were collected at the same stable operating point when the system reached nominal voltage. For this reason, the DPS modulator operates in the SPS state, and the obtained waveforms are identical, proving that the system operates correctly without additional oscillations and disturbances.
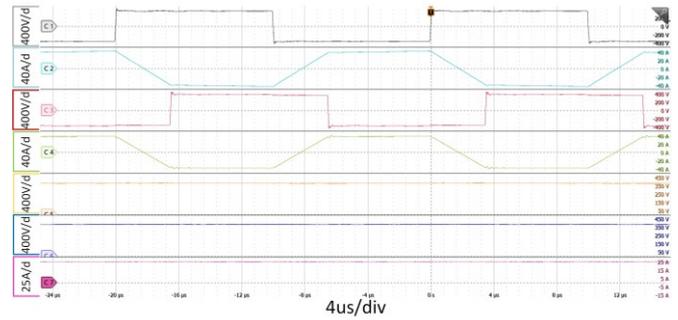
a)
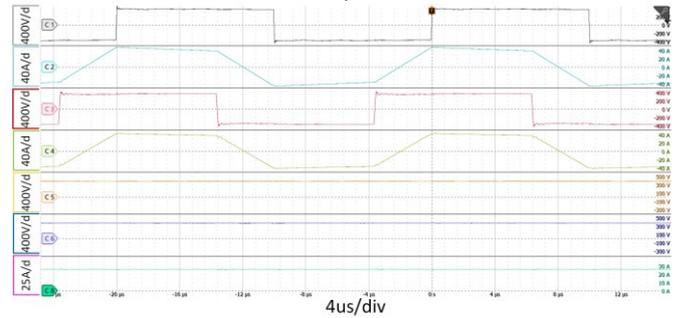
b)

Fig.18. Graph waveform of DAB with SPS modulation, direction flow a) first b) second. From top: C1 - primary phase voltage, C2 - primary phase current, C3 - secondary phase voltage, C4 - secondary phase current,C5 - DC input voltage, C6 - DC output voltage, C7 - DC output load

Subsequently, Figures 19-20 explain the results of dynamic state tests conducted under rated load conditions, offering a comprehensive understanding of the DAB converter's behavior in dynamic scenarios. In the conducted dynamic tests, which required a long time to ramp up, it was necessary to collect samples from several seconds of system operation. To achieve this, it was necessary to limit the quality of the waveforms. Aliasing occurs when an oscilloscope does not sample the signal fast enough to construct an accurate waveform record. Figures 19-20 show the phenomenon of aliasing in the measurement, causing the rising and falling edges of the measurement to appear sinusoidal. It is due our measurement equipment limitation.
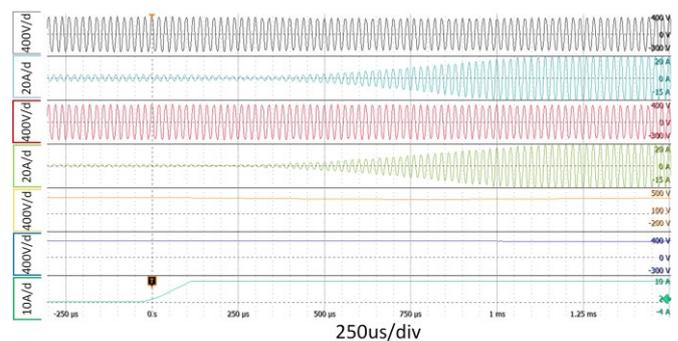

Fig.19. Dynamic state – load step up. From top: primary phase voltage, primary phase current, secondary phase voltage, secondary phase current, DC input voltage, DC output voltage, DC output load

8
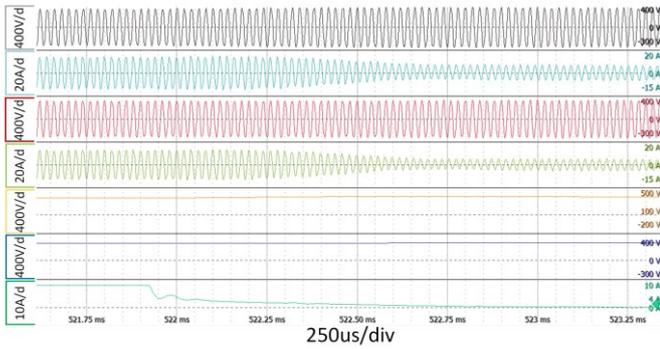
Fig.20. Dynamic state – load step down. From top: primary phase voltage, primary phase current, secondary phase voltage, secondary phase current, DC input voltage, DC output voltage, DC output load

Concluding the analysis, Figures 21-23 encapsulate the outcomes of tests exploring variations in the supply voltage of the DAB converter. This exploration mirrors phenomena similar to those encountered in traction lines, providing valuable insights into the converter's response under varying supply conditions. The meticulous presentation of these test results contributes to a holistic comprehension of the DAB converter's performance characteristics across diverse operational scenarios.

The presented results of dynamic states in Figures 24-25 indicate a step change in voltage within the range of 140-70%. By utilizing the presented solution with an additional phase shift, the phenomenon of DC bias occurring during the step change of phase shift is eliminated. The tests were conducted at half the voltage to ensure the preservation of the maximum voltage.
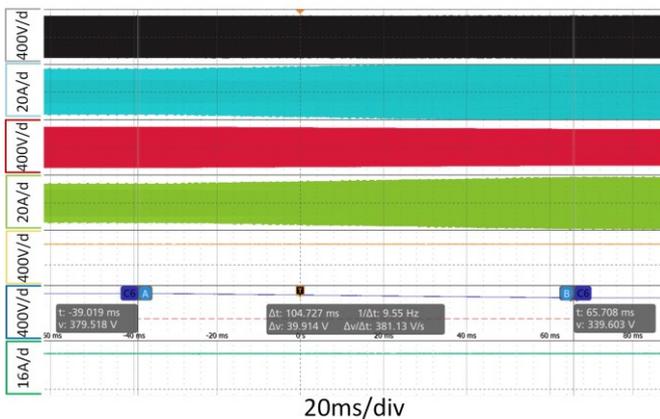

Fig.21. Dynamic state – change of input voltage at nominal run. From top: primary phase voltage, primary phase current, secondary phase voltage, secondary phase current, DC input voltage, DC output voltage, DC output load
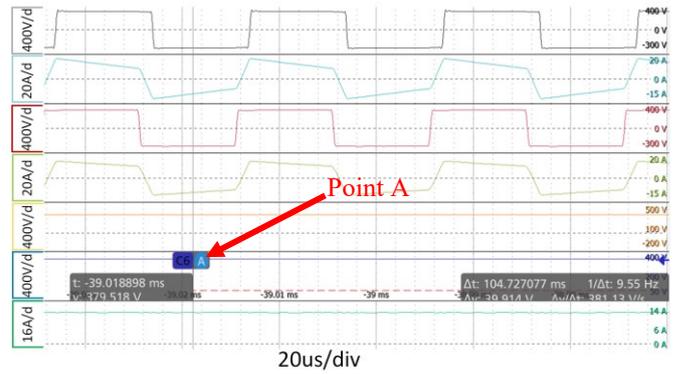

Fig.22. Dynamic state – zoom of point A – change of input voltage at nominal run. From top: primary phase voltage, primary phase current, secondary phase voltage, secondary phase current, DC input voltage, DC output voltage, DC output load
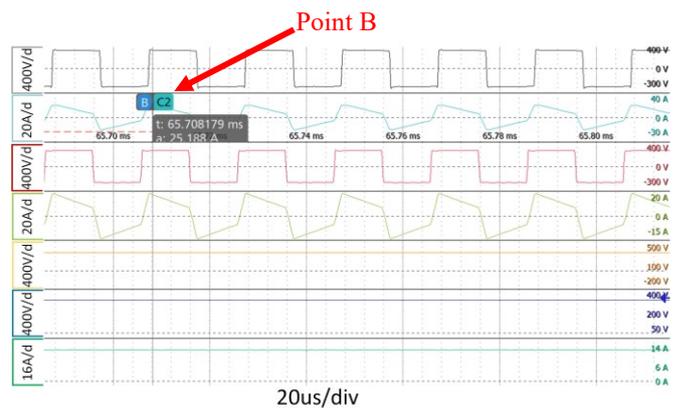
Fig.23. Dynamic state – zoom of point B – change of input voltage at nominal run. From top: primary phase voltage, primary phase current, secondary phase voltage, secondary phase current, DC input voltage, DC output voltage, DC output load
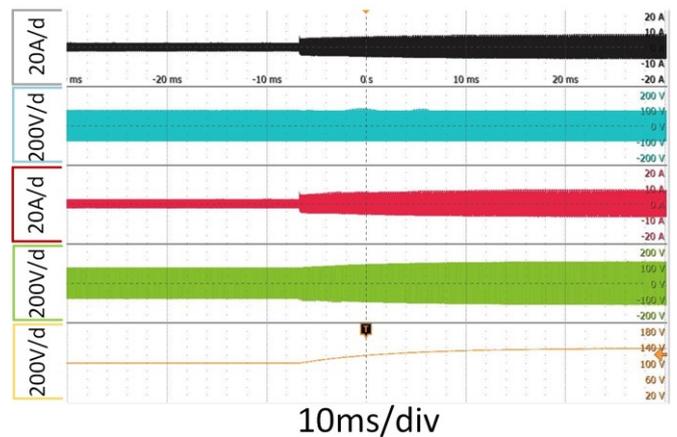

Fig.24. Dynamic state – A step change in voltage within the range of 140% of the rated voltage. From top: primary phase voltage, primary phase current, secondary phase voltage, secondary phase current, DC output voltage

9
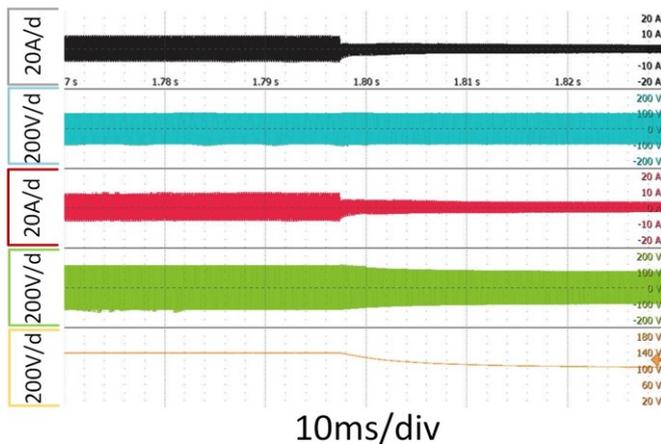
Fig.25. Dynamic state – A step change in voltage within the range of 70% of the rated voltage. From top: primary phase voltage, primary phase current, secondary phase voltage, secondary phase current, DC output voltage

The developed dynamic tests demonstrate a favorable performance characteristic of the system, with the elimination of issues related to current asymmetry or significant drops in DC output voltage. This indicates that the implemented modified DPS modulation method operates correctly in dynamic states, whether during system startup, voltage changes, or dynamic load and set voltage changes.

7. CONCLUSIONS

The article describes a new approach to starting the DAB converter based on modified DPS modulation. The proposed approach has been positively tested in the simulation and laboratory tests and can be successfully used in DC microgrid DAB configurations. The proposed control solution is much simpler to implement, as there is no need to implement very advanced state machines for full DPS/TPS modulation. The solution consists in the implementation of the selected DPS modulation state and works at optimal modulation points, which makes it possible to implement the algorithm in simple DSP and FPGA systems. By taking into account the new design procedure, part of the problems related to the DAB dynamic states has been eliminated. The introduction of changes in the control loop increases the efficiency of the system in relation to the classic control with SPS modulation. The DPS state IV solves the DAB start problem. The system behaves stably under a sudden load change in the range of 0-100% of the rated power when both increasing and decreasing the load. In this case, the settling time of the operating point is ~100 us (rising edge) ~150 us (falling edge), which is a very good result, taking into account the requirements for systems operating in microgrid networks (Figures 20-21).

The proposed control system enables stable operation in the event of a change in the supply voltage in the range of 20% down. Despite changes in the supply voltage, no rapid changes in the values of currents in the system are observed. The applied control method eliminates the need to scale the magnets and diodes, which significantly reduces the cost of building a high-power system.

Future research works will be focused on validation of the presented method in a three-phase DAB converter.

8. REFERENCES

[1] D. Saha et al., "Space Microgrids for Future Manned Lunar Bases: A Review," in IEEE Open Access Journal of Power and Energy, vol. 8, pp. 570-583, 2021, doi: 10.1109/OAJPE.2021.3116674.

[2] Piasecki, S.; Zaleski, J.; Jasinski, M.; Bachman, S.; Turzyński, M. Analysis of AC/DC/DC Converter Modules for Direct Current Fast-Charging Applications. Energies 2021, 14, 6369. https://doi.org/10.3390/en14196369.

[3] Morawiec, M. Lewicki, A. Power electronic transformer based on cascaded H-bridge converter. Bull. Pol. Acad. Sci. Tech. Sci. 2017, 65, 675-683.

[4] Lavanya, A. Jegatheesan R. Vijayakumar K. Navamani J. A comprehensive Review on Bidirectional, Traction Converter for Electric Vehicles, Bull. Pol. Acad. Sci. Tech. Sci. 2019, 65, 635-649.

[5] Jalbrzykowski S. Citko T. A bidirectional DC-DC converter for renewable energy systems. Bull. Pol. Acad. Sci. Tech. Sci. 2009, 57, 363–368.

[6] N. Hou, Y. W. Li and L. Ding, "Communicationless Power Management Strategy for the Multiple DAB-Based Energy Storage System in Islanded DC Microgrid," 2020 IEEE Energy Conversion Congress and Exposition (ECCE), Detroit, MI, USA, 2020, pp. 4656-4661, doi: 10.1109/ECCE44975.2020.9236420.

[7] Turzyński, M.; Bachman, S.; Jasiński, M.; Piasecki, S.; Ryłko, M.; Chiu, H.-J.; Kuo, S.-H.; Chang, Y.-C. Analytical Estimation of Power Losses in a Dual Active Bridge Converter Controlled with a Single-Phase Shift Switching Scheme. Energies 2022, 15, 8262. https://doi.org/10.3390/en15218262.

[8] Barlik, R. Grzejszczak, P. Koszel M. Mathematical and simulation modeling of dual active bridge. Bull. Pol. Acad. Sci. Tech. Sci. 2022, 70, 142–653. DOI: 10.24425/bpasts.2022.142653

[9] Tong, L. Hang, G. Li and J. Huang, "Nonlinear characteristics of DAB converter and linearized control method," 2018 IEEE Applied Power Electronics Conference and Exposition (APEC), San Antonio, TX, USA, 2018, pp. 331-337, doi: 10.1109/APEC.2018.8341031.

[10] J. -i. Itoh, K. Kawauchi and H. Watanabe, "Non-linear Dead-time Error Compensation Method of Dual Active Bridge DC-DC Converter for Variable DC-bus Voltage," 2018 International Conference on Smart Grid (icSmartGrid), Nagasaki, Japan, 2018, pp. 208-213, doi: 10.1109/ISGWCP.2018.8634560.

[11] S. Baba, S. Bachman, M. Jasinski and M. Zelechowski, "WBG-Based PEBB Module for High Reliability Power Converters," in IEEE Access, vol. 9, pp. 86488-86499, 2021, doi: 10.1109/ACCESS.2021.3089045..

[12] Z. Zhu, Y. Zheng, Y. Fang and P. Xu, "Analysis of the startup method for building up DC voltage via body diode rectifying in Dual Active Bridge converter," 2014 International Power Electronics and Application Conference and Exposition, Shanghai, China, 2014, pp. 1407-1410, doi: 10.1109/PEAC.2014.7038071..

[13] P. Kundur et al., "Definition and classification of power system stability IEEE/CIGRE joint task force on stability terms and definitions," in IEEE Transactions on Power Systems, vol. 19, no. 3, pp. 1387-1401, Aug. 2004, doi: 10.1109/TPWRS.2004.825981.

[14] S. Dey, S. S. Chakraborty, S. Singh and K. Hatua, "Design of High Frequency Transformer for a Dual Active Bridge (DAB) Converter," 2022 IEEE Global Conference on Computing, Power and Communication Technologies (GlobConPT), New Delhi, India, 2022, pp. 1-6, doi: 10.1109/GlobConPT57482.2022.9938249..

[15] Z. Zhu, J. Liu, F. Xiao, P. Chen and Q. Ren, "Start-up Procedure and Soft-starting Strategy for Dual Active Bridge Converter," 2020 IEEE 9th International Power Electronics and Motion Control Conference (IPEMC2020-ECCE Asia),

Nanjing, China, 2020, pp. 566-571, doi: 10.1109/IPEMC-ECCEAsia48364.2020.9367737.

[16] Q. Zeng, Y. Wei, B. Yang, J. Xu and D. Zhao, "Research on DAB Triple Phase Shift Control Strategy Based on Current Stress and Soft Switch Dual Objective Optimization," 2021 11th International Conference on Power and Energy Systems (ICPES), Shanghai, China, 2021, pp. 36-41, doi: 10.1109/ICPES53652.2021.9683807..

[17] Barlik, R.; Nowak, M.; Grzejszczak, P.; Zdanowski, M. Analytical description of power losses in a transformer operating in the dual active bridge converter. Bull. Pol. Acad. Sci. Tech. Sci. 2016, 64, 561–574.

[18] Z. Zhu, J. Liu, F. Xiao, P. Chen and Q. Ren, "Start-up Procedure and Soft-starting Strategy for Dual Active Bridge Converter," 2020 IEEE 9th International Power Electronics and Motion Control Conference (IPEMC2020-ECCE Asia), Nanjing, China, 2020, pp. 566-571, doi: 10.1109/IPEMC-ECCEAsia48364.2020.9367737.

[19] D. -D. Nguyen and K. Yukita, "A soft-starting method for Dual Active Bridge Converters," 2019 IEEE Third International Conference on DC Microgrids (ICDCM), Matsue, Japan, 2019, pp. 1-6, doi: 10.1109/ICDCM45535.2019.9232801.

[20] S.Bachman, M. Turzński, M. Jasiński, 'Modern control strategy of bidirectional DAB converter with consideration of control nonlinearity' SENE, Łódź 2023.

[21] X. Liu, M. Han, D. Liu, Z. Li, Z. Dong and Z. Zhang, "A New Start-up Method for Dual Active Bridge Power Converters," 2022 IEEE 5th International Electrical and Energy Conference (CIEEC), Nanjing, China, 2022, pp. 4266-4270, doi: 10.1109/CIEEC54735.2022.9846100.

[22] T. -W. Huang, S. -H. Kuo, C. -C. Wang and H. -J. Chiu, "High Power Dual Active Bridge Converter in Wide Voltage Range Application," 2021 International Conference on Fuzzy Theory and Its Applications (iFUZZY), Taitung, Taiwan, 2021, pp. 1-5, doi: 10.1109/iFUZZY53132.2021.9605081.

[23] A. K. Jain and R. Ayyanar, "PWM control of dual active bridge: comprehensive analysis and experimental verification," 2008 34th Annual Conference of IEEE Industrial Electronics, Orlando, FL, USA, 2008, pp. 909-915, doi: 10.1109/IECON.2008.4758074.

[24] A. K. Jain and R. Ayyanar, "PWM control of dual active bridge: comprehensive analysis and experimental verification," 2008 34th Annual Conference of IEEE Industrial Electronics, Orlando, FL, USA, 2008, pp. 909-915, doi: 10.1109/IECON.2008.4758074.

[25] R. Barlik, M. Nowak, P. Grzejszczak. Power transfer analysis in a single phase dual active bridge, BULLETIN OF THE POLISH ACADEMY OF SCIENCES TECHNICAL SCIENCES, Vol. 61, No. 4, 2013 DOI: 10.2478/bpasts-2013-0088.

[26] Wolski, K.; Grzejszczak, P.; Szymczak, M.; Barlik, R. Closed-Form Formulas for Automated Design of SiC-Based Phase-Shifted Full Bridge Converters in Charger Applications. Energies 2021, 14, 5380. https://doi.org/10.3390/en14175380.

[27] S. Dutta and S. Bhattacharya, "A method to measure the DC bias in high frequency isolation transformer of the dual active bridge DC to DC converter and its removal using current injection and PWM switching," 2014 IEEE Energy Conversion Congress and Exposition (ECCE), Pittsburgh, PA, 2014, pp. 1134-1139, doi: 10.1109/ECCE.2014.6953527.

[28] Gierczynski, M.; Grzesiak, L.M.; Kaszewski, A. Cascaded Voltage and Current Control for a Dual Active Bridge Converter with Current Filters. Energies 2021, 14, 6214. https://doi.org/10.3390/en14196214.

[29] C. Du, W. Guo, S. Guo, W. Cai and Q. Shi, "Transient Current Optimal Control of the Hybrid Three Level Dual Active Bridge Converters Based on Triple-Phase-Shifting Control," 2021 IEEE 12th International Symposium on Power Electronics for Distributed Generation Systems (PEDG), Chicago, IL, USA, 2021, pp. 1-8, doi: 10.1109/PEDG51384.2021.9494170.

[30] J. Xu et al., "Fast Transient Current Control for Dual-Active-Bridge DC-DC Converters with Triple-Phase-Shift," 2019 IEEE Applied Power Electronics Conference and Exposition (APEC), Anaheim, CA, USA, 2019, pp. 2197-2201, doi: 10.1109/APEC.2019.8722187.

[31] G. Yang, D. Zhang, X. Yang and M. Zhang, "Transient DC bias suppression and general dynamic modulation for dual active bridge converter," 2022 IEEE International Power Electronics and Application Conference and Exposition (PEAC), Guangzhou, Guangdong, China, 2022,pp.527532,doi:10.1109/PEAC56338.2022.995912.

[32] L. Jiang, G. Li, M. Yang, W. Sima, X. Wang and S. Ding, "Research on Electromagnetic Transient Model and Control Strategy of Dual Active Bridge Considering Transformer Core Nonlinearity," 2022 IEEE International Conference on High Voltage Engineering and Applications (ICHVE), Chongqing, China, 2022, pp. 1-3, doi: 10.1109/ICHVE53725.2022.9961417.

11